Liquid Crystals
Publication details, including instructions for authors and subscription information:
http://www.informaworld.com/smpp/title~content=t713926090

Mean field theory-based calculation of FLC polarization

Matthew A. Glaser; Noel A. Clark; David M. Walba; Michael P. Keyes; Marc D. Radcliffe; Daniel C. Snustad

Online publication date: 11 November 2010

To cite this Article Glaser, Matthew A. , Clark, Noel A. , Walba, David M. , Keyes, Michael P. , Radcliffe, Marc D. and Snustad, Daniel C.(2002) 'Mean field theory-based calculation of FLC polarization', Liquid Crystals, 29: 8, 1073 — 1085
To link to this Article: DOI: 10.1080/02678290210145256
URL: http://dx.doi.org/10.1080/02678290210145256

LIQUID CRYSTALS, 2002, VOL. 29, NO. 8, 1073–1085

Taylor & Francis
Taylor & Francis Group

Mean field theory-based calculation of FLC polarization

MATTHEW A. GLASER*, NOEL A. CLARK
Department of Physics and Ferroelectric Liquid Crystal Materials Research Center,
University of Colorado, Boulder, Colorado 80309, USA

DAVID M. WALBA
Department of Chemistry and Biochemistry and Ferroelectric Liquid Crystal
Materials Research Center,
University of Colorado, Boulder, Colorado 80309, USA

MICHAEL P. KEYES, MARC D. RADCLIFFE and DANIEL C. SNUSTAD
3M Company, St. Paul, Minnesota 55144, USA

(*Received 7 December 2001; in final form 11 March 2002; accepted 19 March, 2002*)

Mean field theory and Monte Carlo sampling are applied to the calculation of the spontaneous polarization density of ferroelectric liquid crystals by the ensemble averaging of single molecules confined in mean field potentials reflecting the SmC environment. Molecules are modelled with atomistic detail, using intramolecular interaction potentials derived from *ab initio* quantum mechanical calculations. This technique is applied to thirteen members of a family of novel fluoro ether-based compounds. Comparison with experiment shows that the observed variation of polarization density with chemical structure is well reproduced in most cases, but that the observed temperature dependence of polarization density is not captured by our model. The features of molecular organization responsible for the discrepancies between theory and experiment are discussed.

1. Overview

We describe the application of a simple mean field model (The Boulder model [1, 2]) to the calculation of spontaneous polarization density P for a chemically novel family of ferroelectric liquid crystals (FLCs) designed by the 3M Speciality Chemical Division. We have previously applied the Boulder model to the calculation of *saturated* polarization density (i.e. the value of P deep within the SmC* phase) for a chemically diverse group of FLCs, and have demonstrated an encouraging level of correlation between the calculated P values and those measured experimentally [3, 4]. Our earlier study demonstrated that the Boulder model is a useful semi-quantitative predictor of saturated polarization density in FLCs, enabling the pre-synthesis identification of high P ($P \geqslant 100\ \mathrm{nC\,cm^{-2}}$) and low P ($P < 100\ \mathrm{nC\,cm^{-2}}$) FLCs, with only chemical structure required as input. Our earlier study also showed that the Boulder model reproduces the correct *sign* of P in nearly all cases, and appears to be applicable both to single component FLCs and to mixtures of a chiral dopant with an achiral or racemic SmC host.

The present study represents an application of the Boulder model to the calculation of P for a family of FLCs containing highly flexible chiral fluoro ether tails that exhibits low rotational viscosity and a remarkable lack of layer contraction upon entering the SmC phase [5]. This study was conducted as a *blind test* of the Boulder model: with the exception of two compounds whose measured polarization densities have been used to calibrate the model, the measured polarization densities for the FLCs studied here were unknown to us at the time the calculations were carried out. We have also attempted to model the *temperature dependence* of P, rather than just its saturated value, for several of the compounds investigated. Since our earlier study [3, 4], we have substantially modified our computational methodology in an attempt to eliminate sources of systematic error, focusing on the development of improved intramolecular potentials and more accurate charge distributions.

*Author for correspondence;
e-mail: matthew.glaser@colorado.edu

Liquid Crystals ISSN 0267-8292 print/ISSN 1366-5855 online © 2002 Taylor & Francis Ltd
http://www.tandf.co.uk/journals
DOI: 10.1080/02678290210145256

Given the mean field assumptions upon which the Boulder model is based, i.e. that the orientational–conformational probability distribution of single molecules in the SmC phase can be modelled by a simple mean field potential, a high level of quantitative accuracy is perhaps not to be expected. Rather, we hope to capture some of the main *trends* in P with respect to variation of temperature and/or chemical structure, and to provide theoretical insight into the microscopic origins of ferroelectric polarization in FLCs.

2. Methodology

2.1. *The Boulder model*

A comparison of SmC tilt angles derived from optical and X-ray measurements reveals that, quite generally, the optical tilt angle θ_{opt} (the tilt from the layer normal of the axis of the diagonal frame of the optical dielectric tensor) is larger than the X-ray tilt angle θ_{xray} (deduced from the layer shrinkage upon cooling from the SmA phase into the SmC phase [6]). This observation has led to the 'zig-zag' model of SmC ordering [7], in which the aromatic molecular cores (which predominantly determine the birefringence and hence θ_{opt}) are assumed to be more tilted relative to the layer normal than the pendant aliphatic tails, giving less layer shrinkage than would be expected if the entire molecule tilted through θ_{opt} (leading to $\theta_{xray} < \theta_{opt}$). The Boulder model is based upon this intuitive picture of the SmC molecular organization.

An immediate consequence of the zig-zag model is that even an *achiral* SmC phase possesses *intrinsic polar orientational order* (this is, in fact, a general consequence of the symmetry of the SmC phase, independent of any specific microscopic model—see, for example, figure 7.18 in [8]) [1–4, 9, 10]. Consider an idealized molecule having a rigid zig-zag shape, with the LC core associated with the central segment of the zig-zag and the tails with the outboard segments of the zig-zag. The symmetry of the SmC phase implies that a configuration of this molecule in which the core is more tilted relative to the layer normal than the tails occurs with a different probability than a configuration in which the tails are more tilted than the core, obtained from the first configuration by a π rotation of the molecule about its long axis (π rotation about the molecular long axis is not a SmC symmetry).

If we now make the molecule chiral by including an electric dipole normal to the plane of the zig-zag, then it is clear that the dissymmetry between the two configurations described above leads to a net ferroelectric polarization density in the direction normal to the average tilt plane. In the Boulder model, it is this lack of invariance under a π rotation about the average molecular long axis that is responsible for ferroelectricity. The Boulder model further assumes that cores are more tilted than tails in most cases, and that the molecular organization of the chiral SmC* phase is essentially the same as that of the achiral SmC phase. In this picture, ferroelectricity arises from the 'passive' polar orientational ordering of asymmetric charge distributions associated with chiral groups in an *achiral* zig-zag shaped 'binding site'. The effective binding site for a chiral molecule is said to be 'achiral' if its orientational distribution is approximately mirror symmetric (e.g. essentially the same as that for an achiral SmC phase). The conformational distribution of a chiral molecule always lacks mirror symmetry. The Boulder model mechanism for ferroelectric polarization is depicted schematically in figure 1. The Boulder model makes no distinction between FLCs comprising chiral solutes in achiral SmC hosts and neat SmC* materials—the underlying microscopic mechanism for P is the same in both cases.

The *binding site* for single molecules in the SmC or SmC* phase can be regarded as a *mean field* potential, which represents the average potential of mean force exerted on a given molecule by surrounding molecules in a condensed phase. More precisely, the mean field potential can be defined as that external potential which, when acting on a single molecule in vacuum, produces

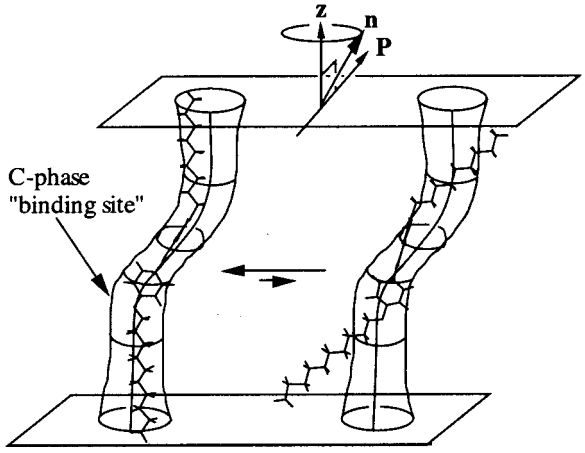

Figure 1. Schematic depiction of the Boulder model mechanism for ferroelectric polarization. In the SmC phase, a rigid, zig-zag shaped molecule resides in a zig-zag shaped mean field potential, or 'binding site'. A molecular configuration that 'adapts' to the binding site (left) has a lower free energy, and hence occurs with a higher probability, than a configuration obtained from the first by a π rotation about the molecular long axis (right), which fits poorly into the binding site. Thus, even in the *achiral* SmC phase, the molecule possesses intrinsic polar orientational order with respect to rotation about the long molecular axis. In the chiral SmC* phase, this polar ordering leads to a macroscopic ferroelectric polarization.

a single-molecule distribution function identical to the single-molecule distribution function in a given condensed phase. Of course, the true single-molecule distribution function in a given liquid crystal (LC) phase is unknown. The success of this approach thus depends on the availability and intelligent use of empirical input to guide the choice of functional form and parametrization of the mean field potential.

For the formulation of *predictive* mean field models for materials properties, another key assumption is that of *microscopic universality*, namely the assumption that the general features of molecular organization in a particular LC phase depend only weakly on the detailed chemical structure of the material in question. This assumption permits the use of a mean field model designed to reproduce the material properties of a known set of LCs to predict variations in those properties with chemical structure. In the present context, microscopic universality is invoked in the assumption of zig-zag ordering for all SmC LCs and in the assumption that a given mean field parametrization can be applied to all members of a chemical family. Systematic studies such as the present one are valuable because they provide a direct test of the microscopic universality assumption, allowing us to define its limits of validity.

An effective mean field model must be both flexible and simple. In other words, it must have enough parameters adequately to represent molecular organization, but no more. To date, we have utilized a simple modular mean field potential similar to those that have been used successfully to model NMR measurements of microscopic order parameters in nematic LCs [11–13]. In this approach, the mean field potential is written as a sum of orientational potentials acting on each rigid molecular segment, which tend to orient the segment along an average symmetry axis. The LC core is treated as a single rigid segment acted upon by an orientational potential, and each bond segment between heavy atoms in the flexible tails is subjected to a separate orientational potential. In its simplest form, our mean field potential for the SmC phase depends on just three parameters, which makes it convenient for routine evaluation of FLC materials.

Note that the full single-molecule distribution function (and thus the full mean field potential) for a smectic LC depends on the position of the molecule relative to the centre of the layer (its Z-coordinate) as well as on molecular orientation and conformation. However, since the observable of interest (P) depends only on molecular orientation and conformation, we are free to work with the effective mean field potential obtained by integrating out the Z-dependence of the full singlet distribution function.

In the mean field approach, the statistical average of any quantity $A(\mathbf{r}^N)$ is given by

$$\langle A \rangle = Z^{-1} \int \mathrm{d}\mathbf{r}^N A(\mathbf{r}^N) \exp(-\beta[V_{\mathrm{int}}(\mathbf{r}^N) + V_{\mathrm{mf}}(\mathbf{r}^n)]) \tag{1}$$

where

$$Z = \int \mathrm{d}\mathbf{r}^N \exp(-\beta[V_{\mathrm{int}}(\mathbf{r}^N) + V_{\mathrm{mf}}(\mathbf{r}^N)]) \tag{2}$$

is the configurational partition function. N is the number of intramolecular atomic sites, $\mathbf{r}^N$ denotes the set of atomic coordinates, V_{int} is the intramolecular potential energy, V_{mf} is the mean field potential, and $\beta = (k_{\mathrm{B}}T)^{-1}$. Our mean field potential for the SmC phase has the form:

$$V_{\mathrm{mf}}(\mathbf{r}^N) = -\sum_{i=1}^{N_{\mathrm{s}}} u_0 |\mathbf{v}_{\mathrm{i}}| P_2(\hat{\mathbf{v}}_{\mathrm{i}} \cdot \hat{\mathbf{n}}_{\mathrm{t}}) - u_0 |\mathbf{v}_{\mathrm{c}}| P_2(\hat{\mathbf{v}}_{\mathrm{c}} \cdot \hat{\mathbf{n}}_{\mathrm{c}}) - \alpha |\mathbf{v}_{\mathrm{ee}}|. \tag{3}$$

The first term in equation (3) is a sum of orientational potentials acting on N_{s} individual bond segments $\mathbf{v}_{\mathrm{i}}$ in the tails, where $P_2(x) = (3x^2 - 1)/2$ is the second Legendre polynomial and $\hat{\mathbf{v}}_{\mathrm{i}} = \mathbf{v}_{\mathrm{i}}/|\mathbf{v}_{\mathrm{i}}|$. This term tends to orient tail segments along the tail 'director' $\hat{\mathbf{n}}_{\mathrm{t}}$, without regard to polarity. The second term represents an orientational potential acting on the molecular core, defined as the ring-containing portion of the molecule, where $\mathbf{v}_{\mathrm{c}}$ is the core end-to-end vector, and $\hat{\mathbf{v}}_{\mathrm{c}} = \mathbf{v}_{\mathrm{c}}/|\mathbf{v}_{\mathrm{c}}|$. This potential tends to orient the core along the core 'director' $\hat{\mathbf{n}}_{\mathrm{c}}$, which is not, in general, parallel to the tail director $\hat{\mathbf{n}}_{\mathrm{t}}$ in the biaxial SmC phase. The strength of individual terms in the orientational potential scales with segment length ($|\mathbf{v}_{\mathrm{i}}|$ or $|\mathbf{v}_{\mathrm{c}}|$), but otherwise depends on a single energy parameter u_0. The third term in equation (3) is a potential that tends to elongate the molecule, where $\mathbf{v}_{\mathrm{ee}}$ is the molecular end-to-end vector. This term is added to counter the tendency of an isolated molecule to adopt folded configurations. Although our neglect of attractive intramolecular van der Waals interactions (see below) reduces this tendency, such an elongational potential is still needed to suppress folded molecular conformations. However, the results do not depend sensitively on α.

Including distinct core and tail directors $\hat{\mathbf{n}}_{\mathrm{c}}$ and $\hat{\mathbf{n}}_{\mathrm{t}}$ in the mean field potential allows us to represent, in a minimal way, the 'zig-zag' character of the SmC binding site. The model depends on three parameters: the overall orientational energy parameter, u_0, the angle between core and tail directors, $\theta_{\mathrm{rel}} = \cos^{-1}(\hat{\mathbf{n}}_{\mathrm{c}} \cdot \hat{\mathbf{n}}_{\mathrm{t}})$, and the elongational energy parameter, α. If cores are assumed to be more tilted than tails in the SmC phase, then

$\hat{\mathbf{n}}_t \times \hat{\mathbf{n}}_c \| \hat{\mathbf{z}} \times \hat{\mathbf{n}}$, where $\hat{\mathbf{z}}$ is the layer normal and $\hat{\mathbf{n}}$ is the average molecular director, so $\hat{\mathbf{n}}_t \times \hat{\mathbf{n}}_c$ defines the direction of positive P, according to the usual convention.

2.2. *Molecular models*

As mentioned above, mean field modelling of LCs requires an accurate expression for the intramolecular potential energy, V_{int}. The general functional form of V_{int} and the procedures used to parametrize V_{int} have been described previously [14]. V_{int} contains both valence (bond stretch, bond angle bend, and dihedral torsion) interaction terms and non-bonded (van der Waals and Coulomb) interaction terms. Because the ferroelectric polarization density depends sensitively on the single-molecule conformational distribution, it is important to incorporate accurate potentials for dihedral torsions about single bonds into our molecular models. We rely on *ab initio* molecular orbital calculations to derive torsional potentials for use in our mean-field calculations. Moderate-level *ab initio* calculations have been shown to yield torsional potentials in good agreement with gas-phase electron diffraction and spectroscopic measurements (see, for example, [15]).

The large number of atoms in most LC molecules precludes their direct study with moderate- to high-level *ab initio* methods, so we generally develop classical interaction potentials (molecular mechanics force fields) based on quantum chemical studies of smaller substructures of LC molecules. Energies of optimized structures are calculated as a function of dihedral angle at the MP2/6-31G(d)//HF/6-31G(d) level using Gaussian 94 [16] (this notation signifies that geometries were optimized at the HF/6-31G(d) level, while single-point energies were calculated at the MP2/6-31G(d) level). The resulting *ab initio* torsional potentials are then fitted to a classical intramolecular potential function.

We utilize 'hybrid' molecular models in which hydrogens attached to sp^2 hybridized carbon atoms are represented as explicit interaction sites, while hydrogens attached to sp^3 carbons are absorbed into 'effective' or 'united' atoms (e.g. methylene and methyl groups are treated as single interaction sites). CF_2 and CF_3 groups are also treated as effective atoms, but a single F atom attached to an sp^3 carbon atom (e.g. at a stereocentre) is included explicitly. The use of effective atoms greatly expedites the calculation of statistical averages.

Equilibrium bond lengths and bond angles are set equal to the corresponding bond lengths and angles in the minimum-energy *ab initio* structure. Generic (Dreiding II [17]) values are used for the bond stretching and bond angle bending force constants. Van der Waals parameters are taken from the literature. Where possible, parameters optimized to reproduce liquid phase thermophysical data are used. In particular, we rely heavily on parameters from OPLS (Optimized Potentials for Liquid Simulations [18–21]), but selected parameters are taken from other sources, specifically for fluorine [22], CH_2 and CH_3 [23], and CF_2 and CF_3 [24].

The long range attractive part of the intramolecular van der Waals interaction is neglected, using the Weeks–Chandler–Andersen separation of the pair potential into attractive and repulsive parts [25]. This is done to help prevent folding of LC molecules due to attractive intramolecular interactions, an undesirable artifact arising from the fact that we simulate single molecules in vacuum. For similar reasons, intramolecular Coulomb interactions are neglected.

Torsional potentials are fitted to a Fourier cosine series in the dihedral angle including up to 12th order terms. A relatively high order Fourier expansion is needed to obtain reasonable fits to the highly structured torsional potentials of some fluorinated alkyl and alkyl ether compounds.

Owing to the neglect of intramolecular Coulomb interactions, site charges are not required for the calculation of V_{int}. However, the molecular charge distribution is needed for the calculation of ferroelectric polarization. Procedures used to obtain charge distributions are described below.

2.3. *Details of calculations*

The ferroelectric polarization density P is related to the component of the average molecular dipole moment $\langle\mu\rangle$ normal to the tilt plane, $\langle\mu_\perp\rangle = \langle\mu\rangle\ \hat{\mathbf{y}}$, where $\hat{\mathbf{y}} = (\hat{\mathbf{n}}_t \times \hat{\mathbf{n}}_c)/|\hat{\mathbf{n}}_t \times \hat{\mathbf{n}}_c|$, via

$$P = n\langle\mu_\perp\rangle, \tag{4}$$

where n is the molecular number density.

The average molecular dipole moment $\langle\mu_\perp\rangle$ is calculated by averaging over all molecular conformations and orientations in a specified mean field potential V_{mf}, as indicated in equation (1). This high-dimensional configurational integral cannot be evaluated directly, so Monte Carlo (MC) methods are used to compute statistical averages. A convenient Monte Carlo scheme for molecular materials is hybrid Monte Carlo (HMC), in which short molecular dynamics (MD) simulations are used to propose MC moves. HMC gives rapid configurational sampling for flexible molecules, while generating states consistent with a canonical ensemble. The specific HMC method used here (described in detail in [3, 4]) is characterized by a high acceptance probability (greater than 90%) and efficient configurational sampling (with 2.6 ps MD trajectories, nearly half of the configurations generated are statistically independent, as measured by the polarization density autocorrelation function).

Calculation of the ferroelectric polarization density requires an accurate representation of the molecular charge distribution. The procedure used in this study differs from that described previously [3] in that we derive charge distributions from *ab initio* quantum mechanical calculations rather than from the empirical 'charge equilibration' method of Rappe and Goddard [26], which is known to give unreliable results in some cases [14]. We determine site charges from ESP fits, that is by fitting the electrostatic potential calculated from *ab initio* charge densities to a site charge model, with the site charges as fitting parameters. For carrying out the ESP fits, we use a robust version of ESP, CHELPG [27].

As discussed above, our simulations utilize a hybrid molecular model, in which some hydrogen and fluorine atoms are combined with the carbon atoms to which they are bonded to form 'united' atoms, which are treated as single interaction sites. However, this procedure also removes the dipole moments associated with the C–H and C–F bonds, which can be substantial in some cases (particularly for C–F bonds). We therefore map effective atom molecular configurations into configurations with all atoms represented explicitly, by adding H and F atoms with the correct local geometry and with appropriate partial charges. This procedure is carried out for every configuration from the HMC simulations for the polarization density calculations.

We utilize charge distributions obtained from moderate-level *ab initio* calculations in the computation of FLC polarization. As such calculations are not feasible for large molecules, we typically carry out *ab initio* calculations for substructures containing the chiral centre and those nearby functional groups considered to be within the chiral 'sphere of influence' of the asymmetric group. Site charges derived from ESP fits to the resulting electron densities are then mapped onto FLC compounds (with site charges for portions of the FLC molecule not spanned by the relevant substructure set to zero) for the calculation of ferroelectric polarization. The implicit assumption here is that only polar groups relatively close to the chiral centre contribute to the polarization.

The remaining issue that must be addressed before applying the Boulder model to the calculation of P is that of *calibration*, namely arriving at a procedure for fixing the parameters in the model (u_0, θ_{rel}, and α). As mentioned above, we found that the calculated values of P were not very sensitive to α. For small α we observe that a significant fraction of molecular configurations are folded (with one tail folded back on itself) which leads to a somewhat reduced average P and large fluctuations in P. We feel that such folded configurations (which are only weakly suppressed by the orientational potential) are unphysical, and in a real LC environment would be strongly suppressed by excluded volume constraints. We thus chose a moderate value of α, $\alpha = 0.15$ kcal mol^{-1} Å^{-1}, which is sufficient to eliminate most folded configurations, but not so large as to restrict the conformational mobility of the flexible tails.

To simplify parametrization of the mean field potential further, we set $\theta_{rel} = \theta_{opt}$, the measured optical tilt angle. Roughly speaking, we assume that the tails are, on average, oriented along the layer normal, while the cores are tilted by θ_{opt} with respect to the layer normal. We are free to do this in the present case because measured optical tilt angles as a function of temperature are available for all compounds except one. The range of variation of θ_{opt} in the present case is not large, however, so the results would not be significantly different if a constant relative tilt angle (say $\theta_{rel} = 30°$) were used for all compounds and temperatures.

Once α and θ_{rel} are fixed, the sole remaining free parameter is u_0. We typically fix u_0 by fitting calculated quantities to experimental measurements. For example, fits to NMR or polarized IR measurements of orientational order parameters can be used to fix u_0, where such measurements are available. Here, we fix u_0 by fitting the calculated polarization to the measured P for two members of the family of 3M materials considered here (see below).

Finally, we note that special care has been taken to estimate the uncertainty in the calculated P, by computing the number of statistically independent measurements in a given HMC run from the polarization density autocorrelation function (see, for example, [28]). We carry out HMC runs of sufficient duration that uncertainties in calculated polarization densities are less than 10 nC cm^{-2} at the one-σ level (68% confidence level). Production runs of ~40 000 HMC steps are sufficient to achieve this level of precision for the FLC materials studied here.

3. Compounds studied

We studied 13 FLC compounds synthesized by the 3M Speciality Chemicals Division. The chemical structures and absolute configurations of these compounds are shown in figure 2. All materials have a phenylpyrimidine core, an achiral alkoxy tail attached to the pyrimidine ring (with the exception of (R)7422[7F8-], which has an alkyl tail), and a highly fluorinated chiral polyether tail attached to the phenyl ring. The chiral tails consist of a fluoro ether segment (in most cases the '422' segment $OCH_2CF_2OC_2F_4OC_4F_9$) separated from the core by a chiral alkyl or alkyl ether spacer. The asymmetric carbon has a single fluoro substituent.

To parametrize a force field for the 3M compounds shown in figure 2, we make use of *ab initio* torsional potentials and equilibrium geometries for the 21 substructures shown in figure 3. The *ab initio* torsional

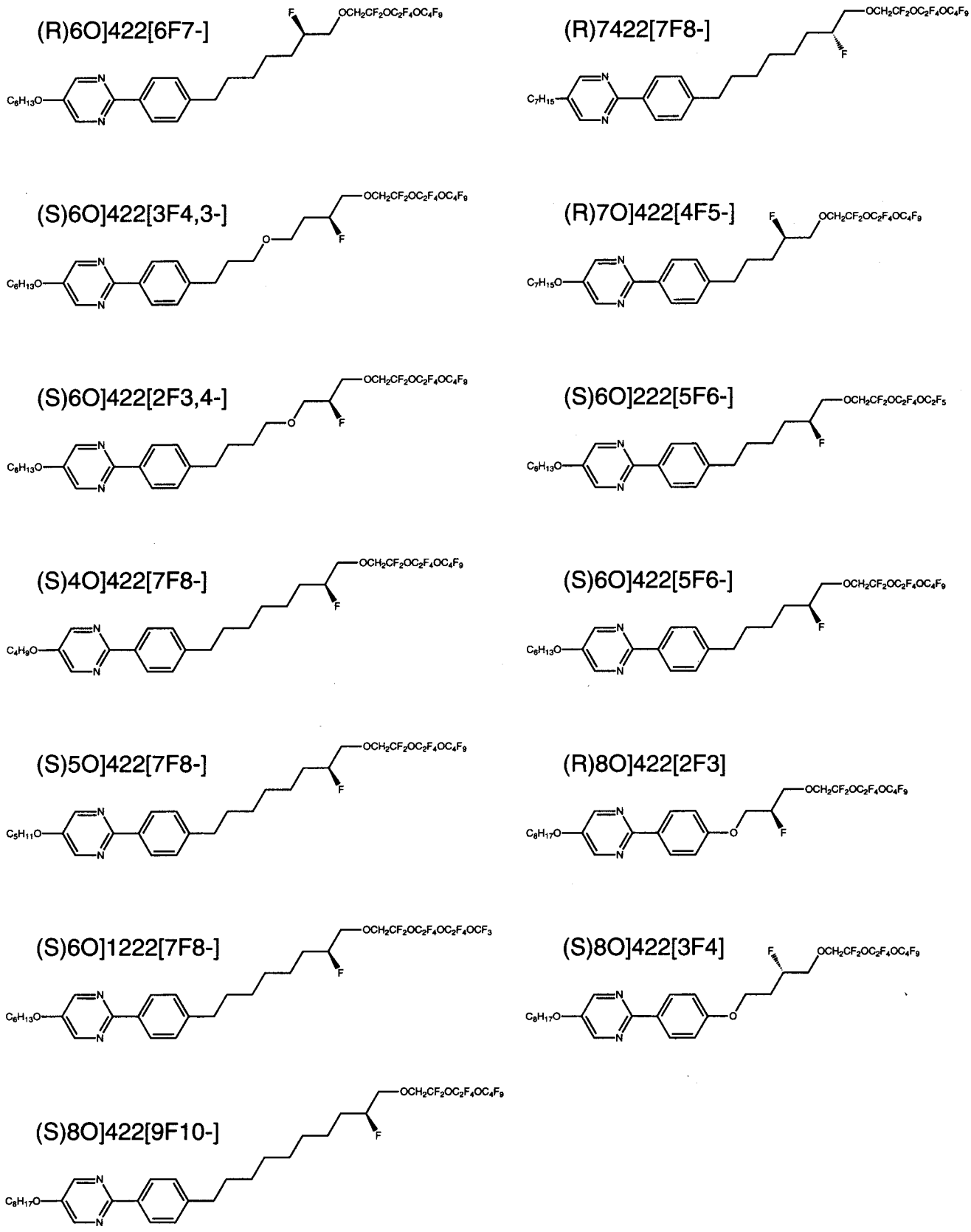

Figure 2. Chemical structures and absolute configurations of the 13 FLC compounds included in this study.

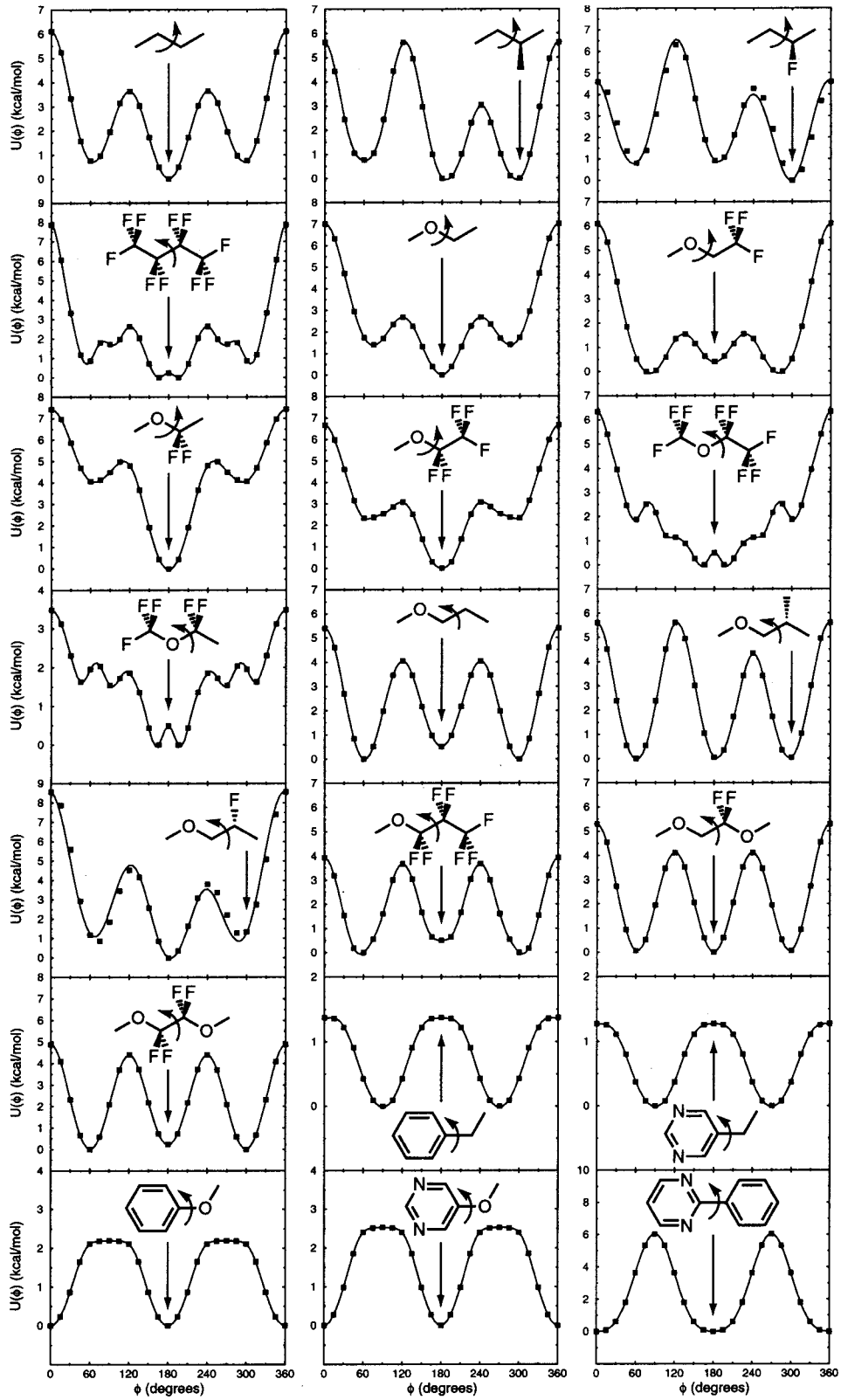

Figure 3. Chemical structures and torsional potentials for rotation about the indicated single bond for the 21 substructures used to parametrize the intramolecular interaction potential used in the calculations. For each substructure, the dihedral angle corresponding to the conformation shown is indicated. Both *ab initio* (squares) and fitted (solid line) torsional potentials are shown.

potentials are shown in figure 3, together with the corresponding force field torsional potentials obtained from fits to the *ab initio* energies. In most cases, the *ab initio* and force field torsional potentials are indistinguishable.

As the mass densities for the materials studied here have not been measured, we assume a constant mass density of $\rho = 1.4\ \mathrm{g\,cm^{-3}}$ for all compounds. This value is in the range measured for similar highly fluorinated LC materials [29]. HF site charge distributions for the 13 3M FLC molecules are obtained from CHELPG ESP fits to HF/6-31G(d) charge densities for the three substructures shown in figure 4.

We fix u_0 by fitting the calculated P_{calc} to the measured P for the two materials for which we have experimental polarization values, (S)6O]222[5F6-] and (S)6O]1222[7F8-]. The measured ferroelectric polarization densities and optical fit angles for (S)6O]222[5F6-] and (S)6O]1222[7F8-] used in determining u_0 are listed in table 1. For these two compounds, we carry out calculations of P for a range of u_0 values, and fit $P_{\mathrm{calc}}(u_0)$ to a straight line with zero intercept (a linear dependence of P on u_0 is assumed). The variation of P_{calc} with u_0 for (S)6O]222[5F6-] and (S)6O]1222[7F8-] is shown in figure 5, together with the linear fits to the data.

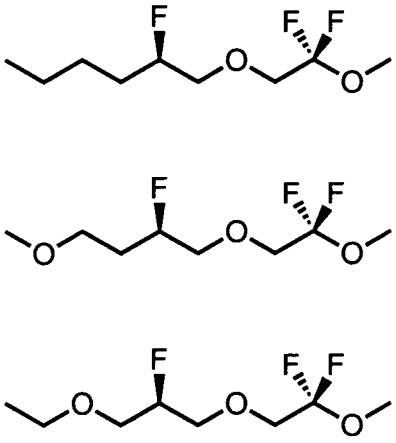

Figure 4. Chemical structure and absolute configuration of FLC substructures for which HF charge distributions were computed. The resulting site charges were used in the calculation of ferroelectric polarization densities.

Table 1. Experimental optical tilt angles θ_{opt} and ferroelectric polarization densities P_{exp} for the two materials used to calibrate the Boulder model. T_{AC} is the SmA–SmC transition temperature.

Compound	T/ °C	$T - T_{\mathrm{AC}}$/ °C	θ_{opt}/ °C	$\mathbf{P}_{\mathrm{exp}}$/ nC cm^{-2}
(S)6O]222[5F6-]	40	−30	23.9	+61.1
(S)6O]1222[7F8-]	46	−29	24.4	+35.5

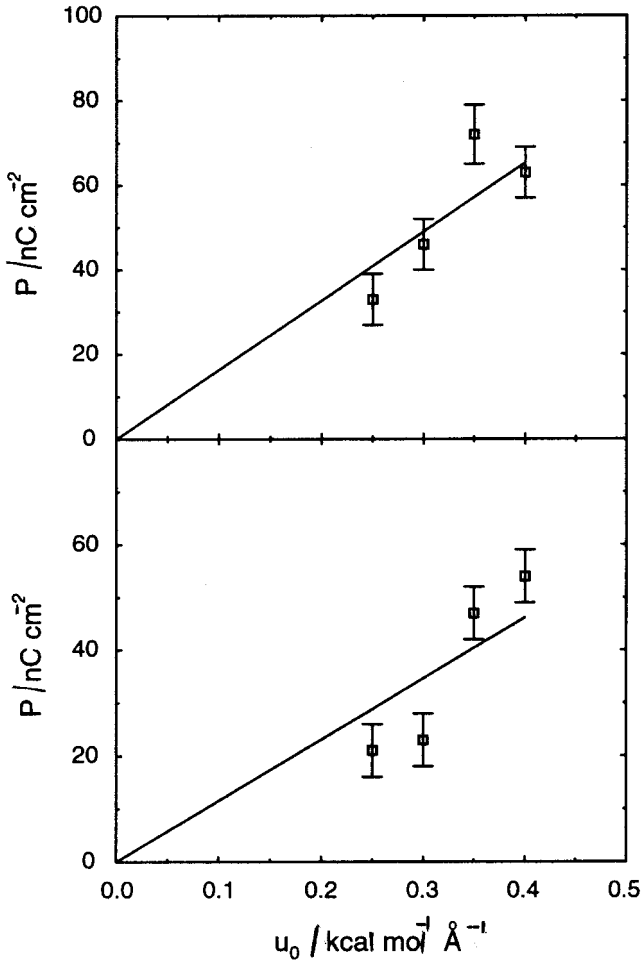

Figure 5. Top: calculated polarization density of (S)6O]222-[5F6-] as a function of u_0 for $\alpha = 0.15$ kcal mol^{-1} Å^{-1}, $\theta_{\mathrm{rel}} = \theta_{\mathrm{opt}} = 23.9°$ and $T = 40°$C (symbols). Bottom: calculated polarization density of (S)6O]1222[7F8-] as a function of u_0 for $\alpha = 0.15$ kcal mol^{-1} Å^{-1}, $\theta_{\mathrm{rel}} = \theta_{\mathrm{opt}} = 24.4°$ and $T = 46°$C (symbols). The solid lines are linear fits to the data with zero intercept.

A best fit value of u_0 is obtained by solving the implicit equation $P_{\mathrm{fit}}(u_0) = P_{\mathrm{exp}}$ for both compounds. For (S)6O]222[5F6-], we find $u_0 = 0.37$ kcal mol^{-1} Å^{-1}, while for (S)6O]1222[7F8-] we find $u_0 = 0.31$ kcal mol^{-1} Å^{-1}. In the remaining calculations, we use the average of the two values, $u_0 = 0.34$ kcal mol^{-1} Å^{-1}.

4. Results

The experimental and calculated ferroelectric polarization densities (P_{exp} and P_{calc}, respectively) for the 13 FLC materials studied here are listed in table 2, together with the temperatures at which the HMC simulations were carried out and the values of $\theta_{\mathrm{rel}} = \theta_{\mathrm{opt}}$ used in the calculations. Also listed are the average nematic order parameters of the *para*-axes of pyrimidine and phenyl

Table 2. Experimental (P_{exp}) and calculated (P_{calc}) ferroelectric polarization densities for the compounds and temperatures listed in the table. T_{AC} is the SmA–SmC transition temperature. All calculations were carried out for $u_0 = 0.34$ kcal mol^{-1} Å^{-1}, $\alpha = 0.15$ kcal mol^{-1} Å^{-1}, and $\theta_{rel} = \theta_{opt}$, for the listed values of θ_{opt}. Also listed are the average nematic order parameters of the *para*-axes of pyrimidine and phenyl rings, S_{pyr} and S_{ph}, respectively. S_{pyr} and S_{ph} are measured in the average symmetry frame of the phenylpyrimidine core. The experimentally measured optical tilt angles θ_{opt} was used in the calculation of P for all compounds except (R)7422[7F8-], for which a tilt angle $\theta_{opt} = 30°$ was assumed.

Compound	T/°C	$T - T_{Ac}$/°C	θ_{opt}/°C	P_{exp}/nC cm^{-2}	P_{calc}/nC cm^{-2}	S_{pyr}	S_{ph}
(R)6O]422[6F7-]	66	−38	32.6	+38.5	+34±4	0.82	0.82
(S)6O]422[2F3,4-]	31	−30	24.8	+27.5	+36±5	0.83	0.82
(S)6O]422[3F4,3-]	50	−20	29.1	+27.9	+15±5	0.81	0.81
	40	−30	29.8	+34.6	+21±5	0.82	0.81
	20	−50	30.1	+49.2	+14±6	0.83	0.83
	0	−70	29.8	+65.4	+13±7	0.84	0.83
(S)8O]422[9F10-]	77	−20	27.9	+20.5	+31±4	0.80	0.80
	57	−40	28.4	+25.2	+35±4	0.81	0.81
	37	−60	28.0	+30.8	+40±5	0.82	0.82
(S)4O]422[7F8-]	60	−10	26.5	+39.4	+38±5	0.80	0.80
	50	−20	29.3	+57.2	+41±5	0.81	0.80
(S)5O]422[7F8-]	60	−10	25.2	+28.9	+45±5	0.80	0.80
	50	−20	27.3	+36.4	+33±5	0.80	0.80
	40	−30	28.8	+47.2	+44±5	0.81	0.80
	30	−40	30.2	+66.8	+46±6	0.81	0.81
(R)7O]422[4F5-]	22	−28	18.8	+1.9	+25±4	0.85	0.85
(R)8O]422[2F3]	61	−35	35.4	+159.0	+35±6	0.79	0.79
(S)6O]222[5F6-]	40	−30	23.9	+61.1	+63±6	0.81	0.81
(S)6O]422[5F6-]	58	−30	30.0	+52.2	+55±5	0.80	0.80
(S)8O]422[3F4]	54	−30	20.8	−18.5	−15±5	0.84	0.84
(S)6O]1222[7F8-]	46	−29	24.4	+35.5	+51±6	0.82	0.81
(R)7422[7F8-]	28	−30	(30.0)	−34.6	−45±6	0.82	0.81

rings, S_{pyr} and S_{ph}, respectively. S_{pyr} and S_{ph} are measured in the average symmetry frame of the phenylpyrimidine core (and thus correspond to the order parameters that would be measured in an NMR experiment). A more immediate impression of the overall level of agreement between theory and experiment may be obtained from figure 6, where P_{calc} is plotted against P_{exp}.

Note that the correct sign of P is predicted by the model in every case, and that most of the data points cluster around the line $P_{calc} = P_{exp}$ (dashed line), which indicates that the Boulder model generally captures the correct molecule-scale physics. There are obvious outliers, however, including (R)8O]422[2F3], for which $P_{calc} = +35 \pm 6$ nC cm^{-2} and $P_{exp} = +159$ nC cm^{-2}, (R)7O]422[4F5-], for which $P_{calc} = +25 \pm 4$ nC cm^{-2} and $P_{exp} = +1.9$ nC cm^{-2}, and (S)6O]422[3F4,3-], which exhibits an increasing deviation from the line $P_{calc} = P_{exp}$ with decreasing temperature. In fact, our model fails to capture the correct temperature dependence of P for all compounds for which the variation of P_{exp} with temperature was measured. The calculated polarization densities are consistent (to within uncertainty) with a temperature-independent polarization density, whereas P_{exp} exhibits a strong temperature dependence in all cases. A possible exception is (R)8O]422[2F3], for which the temperature dependence of P_{calc} appears to follow that of P_{exp}. We consider this apparent agreement with experiment to be fortuitous, however, as P_{calc} can be assumed to be constant to within uncertainty.

The calculated polarization densities are in all cases smaller in magnitude than 100 nC cm^{-2}. This is not surprising, given that the chiral centre is relatively distant from the core–tail junction in most compounds. In the Boulder model, the anisotropy of the orientational distribution about the molecular long axis (polar orientational ordering) for specific functional groups is most pronounced near the core–tail junction, as this is where the 'zig-zag' potential (the difference in the preferred orientation of the core relative to that of the tail) is most strongly expressed. The conformational mobility of the tail causes this anisotropy to become washed out as one moves out along the tail from the core, and so P generally decreases as the chiral centre and associated polar groups move further out on the tail.

In all cases, the sign of the P_{calc} is consistent with the 'naive' Boulder model, assuming that the dipole associated with the C–F bond at the chiral centre makes a majority contribution to P (whether this is true or not will be discussed below). Examination of figure 2 reveals that for every compound except (S)8O]422[3F4] and

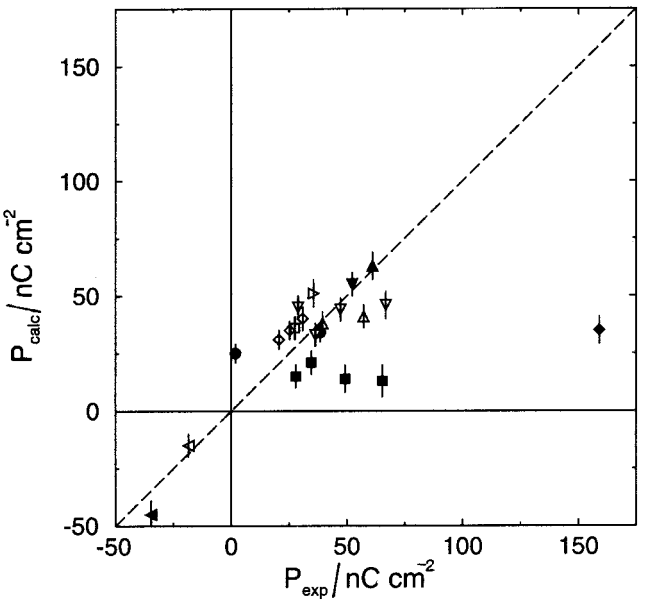

Figure 6. Scatter plot of calculated vs experimental polarization densities for (R)6O]422[6F7-] (open circle), (S)6O]422[2F3,4-] (open square), (S)6O]422[3F4,3-] (filled squares), (S)8O]422[9F10-] (open diamonds), (S)4O]422[7F8-] (open up triangles) (S)5O]422[7F8-] (open down triangles), (R)7O]422[4F5-] (filled circle), (R)8O]422[2F3] (filled diamond), (S)6O]222[5F6-] (filled up triangle), (S)6O]422[5F6-] (filled down triangle), (S)8O]422[3F4] (open left triangle), (S)6O]1222[7F8-] (open right triangle), and (R)7422[7F8-] (filled left triangle). Most data points cluster near the line $P_{calc} = P_{exp}$ (dashed line), although there are some outliers.

(R)7422[7F8-] the C–F dipole moment has a component *into* the plane of the page, while for these two compounds the C–F dipole moment has a component *out of* the plane of the page. Assuming that tails are more tilted than cores, and that the most probable molecular conformation is the all-*trans* conformation shown in figure 2, we would predict a positive polarization for all compounds except (S)8O]422[3F4] and (R)7422[7F8-], a prediction that is borne out by the calculated values in table 2.

As mentioned above, for the four compounds for which P was calculated as a function of T ((S)6O]422-[3F4,3-], (S)8O]422[9F10-], (S)4O]422[7F8-], and (S)5O]422[7F8-]) there is essentially *no* variation of P_{calc} with T, to within the estimated uncertainties. This is not too surprising, as the mean field parameters do not vary significantly with temperature. The only possible source of a strong T-dependence in P for our model is an unusually strong dependence of the conformational distribution on temperature. However, a strong thermal variation of the conformational distribution seems unlikely given the small range of temperatures (relative to the absolute temperature) involved.

The Boulder model calculations yield considerably more information than just the average polarization density. For example, we can measure the contribution of specific polar groups to the overall polarization, by decomposing the site charge distribution into bond dipoles, and then measuring the average contribution of specific bond dipole moments to the total polarization density. The results of this analysis are shown in table 3, which lists bond dipole contributions to P_{calc} for the 13 FLC compounds studied here. Results for a single temperature are listed for each compound, as the results are not strongly temperature-dependent. The table lists contributions from bond dipoles that contribute significantly to P_{calc}: the bond dipole associated with the chiral C–F bond, P_{CF}, bond dipoles associated with the ether oxygen two sites beyond the chiral carbon, $P_{CO}^{(1)}$ and $P_{OC}^{(1)}$, and bond dipoles associated with an ether oxygen between the chiral centre and the core (if any), $P_{CO}^{(2)}$ and $P_{OC}^{(2)}$. For the ether polarizations, P_{CO} refers to the C–O bond dipole nearest the core, while P_{OC} refers to the O–C bond on the far side of the ether oxygen relative to the core.

Table 3. Contributions to total ferroelectric polarization density from specific bond dipoles (nC cm^{-2}) for the listed compounds and temperatures. The partial polarization densities listed are defined in the text.

Compound	T/°C	$T - T_{AC}$/°C	P_{CF}	$P_{CO}^{(1)}$	$P_{OC}^{(1)}$	$P_{CO}^{(2)}$	$P_{OC}^{(2)}$	$\Sigma P_{partial}$	P_{calc}
(R)6O]422[6F7-]	66	−38	+54	−22	+2			+34	+34
(S)6O]422[2F3,4-]	31	−30	+43	−20	+7	+15	−7	+38	+36
(S)6O]422[3F4,3-]	0	−70	+29	−13	+1	−3	+1	+15	+13
(S)8O]422[9F10-]	37	−60	+73	−33	+1			+41	+40
(S)4O]422[7F8-]	50	−20	+83	−44	+3			+42	+41
(S)5O]422[7F8-]	30	−40	+103	−51	−4			+48	+46
(R)7O]422[4F5-]	22	−28	+51	−31	+5			+25	+25
(R)8O]422[2F3]	61	−35	+103	−45	+2	−2	−25	+33	+35
(S)6O]222[5F6-]	40	−30	+114	−51	+1			+64	+63
(S)6O]422[5F6-]	58	−30	+108	−53	−2			+53	+55
(S)8O]422[3F4]	54	−30	−26	+16	−2	0	−2	−14	−15
(S)6O]1222[7F8-]	46	−29	+84	−37	+2			+49	+51
(R)7422[7F8-]	28	−30	−106	+55	+7			−44	−45

Evidently, the total polarization for most compounds is essentially the sum of just two bond dipole contributions: P_{CF}, the contribution from the chiral C–F bond dipole, and $P_{CO}^{(1)}$, the contribution from the C–O bond dipole between the carbon atom one site beyond the chiral carbon and the ether oxygen two sites beyond the chiral carbon. In all cases, the two contributions are of opposite sign, and $|P_{CF}|$ is approximately twice as large as $|P_{CO}^{(1)}|$, so the net polarization is about a factor of two smaller than $|P_{CF}|$. For two of the compounds, ((S)6O]422[2F3,4-] and (R)8O]422[2F3]), the bond dipoles associated with an 'in-board' ether oxygen contribute significantly to the total polarization. In both cases, the ether oxygen in question is two sites distant from the chiral carbon. Ether groups more distant from the chiral centre than this do not contribute significantly to P_{calc}. Table 3 also compares the sum of the bond dipole contributions listed in the table, $\Sigma P_{partial}$, with the total calculated polarization density, P_{calc}. In all cases, $\Sigma P_{partial}$ is quite close to P_{calc}, indicating that the dominant contributions to P_{calc} come from the polar groups listed.

The data in table 3 also reveal an even–odd dependence of P on the number of backbone atoms in the chiral spacer. Focusing on P_{CF}, we see that compounds with an even number of backbone atoms in the chiral spacer (those with [2F3], [5F6-], [7F8-], and [9F10-] spacers) have large polarization densities ($|P_{CF}| \sim 100\ nC\,cm^{-2}$) relative to compounds with an odd number of backbone atoms in the chiral spacer (those with [3F4], [4F5-], and [6F7-] spacers), for which $|P_{CF}| \sim 45\ nC\,cm^{-2}$. The two compounds with ether oxygens in the middle of the chiral spacers ((S)6O]422[2F3,4-] and (S)6O]422[3F4,3-]) behave differently, exhibiting relatively small polarizations ($|P_{CF}| \sim 35\ nC\,cm^{-2}$) in spite of the fact that they have an even number of spacer atoms. This is presumably due to the added flexibility imparted to the chain by the ether group: as can be seen from figure 3, there is a high probability of a *gauche* bend about a bond two bonds distant from an ether group in alkyl ethers. With these two exceptions, however, compounds with an even number of backbone atoms in the chiral spacer exhibit either more pronounced polar orientational ordering or a more favourable average orientation of the C–F dipole relative to the polar axis.

Our results show very little dependence of P on the length or type (alkyl vs. alkoxy) of non-chiral tail or on the specific fluoro ether segment (422, 222, or 1222). This is not surprising, given the simple assumptions upon which the Boulder model is based. Within the Boulder model framework, only functional groups within the 'sphere of influence' of the chiral centre (groups to whom the stereo-centre imparts a chiral conformational distribution) contribute directly to P, while more distant groups are significant only to the extent that they modify the degree of polar orientational ordering of groups within the sphere of influence of the chiral centre (typically a weak effect).

The nematic order parameters of the pyrimidine and phenyl rings, S_{pyr} and S_{ph}, respectively, were calculated as a rough check on the reasonableness of the Boulder model parametrization. The calculated order parameters are comparable to those measured for other FLC materials by ^{13}C NMR [30–32], indicating that the value of u_0 used in our calculations is physically reasonable.

5. Discussion

The results presented above demonstrate, that our mean field model for FLC polarization density can serve as a semi-quantitative predictive tool. However, significant discrepancies between theory and experiment are observed for several compounds (notably (R)8O]422[2F3] and (R)7O]422[4F5-]), and the theory fails to reproduce the strong temperature dependence of polarization density exhibited by several materials (namely (S)6O]422[3F4,3-], (S)8O]422[9F10-], (S)4O]422[7F8-], and (S)5O]422-[7F8-]). To understand the disparity between theory and experiment it is necessary to reexamine the assumptions upon which our model is based.

Our model is based on the assumption that the dominant feature of molecular organization in the SmC or SmC* phase is 'zig-zag' ordering (molecular cores more tilted than tails), which induces polar orientational ordering about the molecular long axis. In chiral materials, this polar ordering manifests itself in a spontaneous ferroelectric polarization density. To turn this intuitive idea into a calculation tool, we have formulated a minimal mean field realization of the zig-zag model in which the molecular core and tails are subjected to separate uniaxial orientational potentials with distinct symmetry directions. We have further assumed that a single parametrization of this mean field model can describe the molecular organization of a variety of materials having distinct chemical structures over a range of temperatures (microscopic universality). This assumption, essential to the creation of a predictive model, rests on an underlying assumption that the general features of molecular organization in SmC LCs are largely independent of chemical detail and temperature.

The failure of our model quantitatively to reproduce the measured polarization densities in all cases can be interpreted either as a breakdown of the microscopic universality hypothesis or as an indication that the form of mean field potential considered in this study misses some important features of molecular organization in the 3M family of FLCs. A breakdown of the microscopic universality assumption would imply that the single-molecule distribution function (and hence the effective

mean field potential) depends on chemical structure (and temperature) in a way that cannot be captured by a simple model with a handful of parameters, implying that the development of accurate predictive models for the ferroelectric polarization density is *a priori* impossible. If, on the other hand, the form of the mean field potential is inappropriate, there remains the possibility of evolving accurate predictive models by appropriate modifications in the form of the mean field potential.

To distinguish between these two possibilities and to develop more accurate mean field models requires more information. Fortunately, we have available to us two sources of relevant molecular-scale information: (1) experiments, such as NMR or polarized IR spectroscopy, which probe microscopic order parameters of specific functional groups, and (2) many-molecule atomistic simulations, which give direct access to the single-molecule distribution function (and hence the polarization density), and additionally provide a detailed picture of the molecular-scale organization of LC materials.

Our polarized IR studies of SmC materials have already exposed shortcomings of the 'bare-bones' Boulder model. Specifically, the Boulder model fails fully to account for differences in the apparent tilt angles of specific functional groups ('differential tilt') observed in IR dichroism measurements [33]. The origin of the observed differential tilt lies in an anisotropic orientational distribution of the LC core about its long axis, an effect that is not correctly included in the minimal realization of the Boulder model described above. Although the orientational anisotropy of the core could be treated by including an additional orientational potential in the Boulder model, the IR experiments indicate that the nature of this effect varies strongly from material to material, so that a 'universal' parametrization that takes this effect into account may not be possible. Nevertheless, it is clear that IR data can be used systematically to refine the Boulder model within specific families of FLC materials.

The findings from the polarized IR experiments are supported by our recent large scale simulation studies of a phenyl benzoate-based SmC mesogen, which lends itself to a detailed test of the Boulder model [4]. While the large scale simulations provide strong independent support for the zig-zag model, the orientational distribution of the core about its long axis as measured in the large scale simulations is significantly more anisotropic than the minimal Boulder model predicts. As a consequence, the polar orientational ordering of the first two sites in the LC tails measured by large scale simulation differs significantly from that predicted by the Boulder model, although the Boulder model predictions for the polar ordering of sites more distant from the core are in good accord with large scale simulation. This observation has important implications for the calculation of FLC polarization, as it suggests that Boulder model predictions of P may be significantly in error in cases where the chiral centre is close to the core.

We believe that this effect could explain the large difference between P_{calc} and P_{exp} for (R)8O]422[2F3], in which the chiral centre is on the third site of the asymmetric tail, and the bond dipole associated with the second bond in the tail (the O–C bond) makes a significant contribution to P in the Boulder model calculations (see table 3). For this compound, we may expect a significant error in the Boulder model estimate of $P_{\mathrm{OC}}^{(2)}$, which would lead to a large error in P_{calc}. Similarly, in (R)7O]422[4F5-], another material for which a significant discrepancy between P_{calc} and P_{exp} was noted, the stereo-centre is relatively close to the core.

As discussed above, the failure of our model quantitatively to reproduce the observed temperature dependence of P in the 3M family of FLCs implies that the thermal behaviour of P in these materials is due to effects not included in the Boulder model, and cannot be simply understood in terms of the thermal variation of the conformational distribution for an isolated molecule. This strong temperature dependence is likely to have its origins in the cooperative behaviour of many molecules, which would manifest itself as a strong variation in the form of the 'binding site' as a function of temperature. Without information from other sources, it is difficult to identify the features of molecular organization responsible for such 'anomalous' thermal behaviour and to include these effects in appropriate mean field models. For example, the observed temperature dependence could be due to variations in the orientational distribution of the core about its long axis, arising from thermally driven changes in intermolecular correlations. This possibility could be tested by carrying out polarized IR experiments on homeotropically oriented samples to probe the orientational distribution of the cores about their long axes.

This work was supported by NSF MRSEC Grant DMR 98-09555.

References

[1] Walba, D. M., and Clark, N. A., 1987, *Proc. SPIE*, **825,** 81.
[2] Walba, D. M., 1991, *Adv. Synthe. React. Solids*, **1,** 173.
[3] Glaser, M. A., Ginzburg, V. V., Clark, N. A., Garcia, E., Malzbender, R., and Walba, D. M., 1995, *Mol. Phys. Rep.*, **10,** 26.
[4] Glaser, M. A., 2000, in *Advances in the Computer Simulations of Liquid Crystals*, edited by P. Pasini and C. Zannoni (Kluwer Academic Publishers), pp. 263–331.
[5] Radcliffe, M. D., Brostrom, M. L., Epstein, K. A., Rappaport, A. G., Thomas, B. N., Shao, R., and Clark, N. A., 1999, *Liq. Cryst.*, **26,** 789.

[6] Jang, W. G., Glaser, M. A., Park, C. S., Kim, K. H., Lansac, Y., and Clark, N. A., 2001, *Phys. Rev. E*, **64,** 051712.
[7] Bartolino, R., Doucet, J., and Durand, G., 1978, *Ann. Phys.*, **3,** 389.
[8] De Gennes, P. G., 1974, *The Physics of Liquid Crystals* (Oxford: Clarendon Press).
[9] Photinos, D. J., and Samulski, E. T., 1995, *Science*, **270,** 783.
[10] Terzis, A. F., Photinos, D. J., and Samulski, E. T., 1997, *J. chem. Phys.*, **107,** 4061.
[11] Marcelja, S., 1974, *J. chem. Phys.*, **60,** 3599.
[12] Photinos, D. J., Samulski, E. T., and Toriumi, H., 1991, *Mol. Cryst. liq. Cryst.*, **204,** 161.
[13] Luckhurst, G. R., 1994, *Mol. Phys.*, **82,** 1063.
[14] Glaser, M. A., Clark, N. A., Garcia, E., and Walba, D. M., 1997, *Specta. Acta A*, **53,** 1325.
[15] Allinger, N. L., Fermann, J. T., Allen, W. D., and Schaefer, H. F. III., 1997, *J. chem. Phys.*, **106,** 5143.
[16] Frisch, M. J., Trucks, G. W., Schlegel, H. B., Gill, P. M. W., Johnson, B. G., Robb, M. A., Cheeseman, J. R., Keith, T., Petersson, G. A., Montgomery, J. A. *et al.*, 1995, *Gaussian 94, Revision D.4*, Gaussian, Inc., Pittsburgh PA.
[17] Mayo, S. L., Olafson, B. D., and Goddard, W. A. III., 1990, *J. phys. Chem.*, **94,** 8897.
[18] Jorgensen, W. L., Madura, J. D., and Swenson, C. J., 1984, *J. Am. chem. Soc.*, **106,** 6638.
[19] Briggs, J. M., Matsui, T., and Jorgensen, W. L., 1990, *J. comput. Chem.*, **11,** 958.
[20] Briggs, J. M., Nguyen, T. B., and Jorgensen, W. L., 1991, *J. phys. Chem.*, **95,** 3315.
[21] Jorgensen, W. L., Laird, E. R., Nguyen, T. B., and Tirado-Rives, J., 1993, *J. comput. Chem.*, **14,** 206.
[22] Rappe, A. K., Casewit, C. J., Colwell, K. S., Goddard, W. A. III., and Skiff, W. M., 1992, *J. Am. chem. Soc.*, **114,** 10 024.
[23] Siepmann, J. I., Karaborni, S., and Smit, B., 1993, *Nature*, **365,** 330.
[24] Shin, S., Collazo, N., and Rice, S. A., 1992, *J. chem. Phys.*, **96,** 1352.
[25] Weeks, J. D., Chandler, D., and Andersen, H. C., 1971, *J. chem. Phys.*, **54,** 5237.
[26] Rappe, A. K., and Goddard, W. W. III., 1991, *J. phys. Chem.*, **95,** 3358.
[27] Breneman, C. M., and Wiberg, K. B., 1990, *J. comput. Chem.*, **11,** 361.
[28] Allen, M. P., and Tildesley, D. J., 1987, *Computer Simulation of Liquids* (Oxford: Clarendon).
[29] Rieker, T. P., and Janulis, E. P., 1995, *Phys. Rev. E*, **52,** 2688.
[30] Ho, M.-S., Fung, B. M., Wand, M., and Vohra, R. T., 1993, *Ferroelectrics*, **138,** 51.
[31] Poon, C.-D., and Fung, B. M., 1989, *J. chem. Phys.*, **91,** 7392.
[32] Poon, C.-D., and Fung, B. M., 1989, *Liq. Cryst.*, **5,** 1159.
[33] Matsushima, J., Takanishi, Y., Ishikawa, K., Takezoe, H., Fukuda, A., Park, C. S., Jang, W. G., Kim, K. H., Maclennan, J. E., Glaser, M. A., Clark, N. A., and Takahashi, K., 2002, *Liq. Cryst.*, **29,** 27.